



Winter storm risk assessment in forests with high resolution gust speed data

Thorsten Zeppenfeld¹ · Christopher Jung² · Dirk Schindler² · Holger Sennhenn-Reulen³ · Marie Josefin Ipsen⁴ · Matthias Schmidt¹

Received: 19 October 2022 / Revised: 19 April 2023 / Accepted: 27 April 2023 / Published online: 22 May 2023
© The Author(s) 2023

Abstract

Winter storms pose a major threat to forest management in Central Europe. They affect forests at a large spatial scale and produce large losses in standing and merchantable timber within few hours. The assessment of winter storm vulnerability by statistical modelling serves as an important tool to tackle uncertainties about the damage risk and to inform management decision processes. This study made use of an extensive forest inventory data set from South-West Germany before and after winter storm Lothar in 1999, one of the most severe storm events in Germany over the last decades. Hierarchical logistic models were fitted to relate storm damage probability on individual tree level to features of dendrometry, site, orography, and storm-specific high resolution data of maximum gust speed. We developed two different approaches to implement gust speed as a predictor and compared them to a baseline model with a structured spatial effect function with no gust speed information. Regional and local variability which could not be described by the predictors was modelled by multi-level group effects. Generalisation performance was tested with a spatially and temporally independent data set on storm separation between explicit spatial gust speeds and unknown variability achieved with the parametric multi-level approach led to a higher degree of transparency and utilisability.

Keywords Storm damage probability · Gust speed model · Hierarchical logistic regression · National forest inventory · Vulnerability assessment

Introduction

Windstorms play a dominant role in the disturbance regime of European forests (Seidl et al. 2014). Especially in the season between November and March, extratropical cyclones frequently impact large areas with heavy rainfalls and strong,

energetic wind gusts. Exposed to this threat, forest stands were often severely damaged or replaced in a whole region within few hours. The risk of damage confronts forest owners with a large degree of uncertainty in their management decisions. Hence, an assessment of the vulnerability of their forests to winter storm damage would help to better adapt their goals and actions to mitigate future loss (Hanewinkel et al. 2010).

For vulnerability assessment, it is crucial to understand and quantify the underlying mechanisms which lead to tree damage. However, there are manifold biotic and abiotic factors that are known to have an effect on storm damage (Gardiner 2021). For instance, individual tree features like crown area, root architecture, and height-to-diameter ratio, but also soil rooting depth and exposition of the location do impact storm damage vulnerability. The effectiveness of these factors is hard to grasp because they interact in various complex ways, on different spatial scales, which often result in non-linear behaviour (Messier et al. 2016). Here, modelling could help to break down this complexity by identifying

Communicated by Thomas Knoke.

✉ Thorsten Zeppenfeld
thorsten.zeppenfeld@nw-fva.de

- ¹ Growth & Risk Modelling, Northwest German Forest Research Institute, Grätzelstr. 2, 37079 Göttingen, Germany
- ² Environmental Meteorology, Albert-Ludwigs-University of Freiburg, Werthmannstrasse 10, 79085 Freiburg, Germany
- ³ Information Technology & Biometrics, Northwest German Forest Research Institute, Grätzelstr. 2, 37079 Göttingen, Germany
- ⁴ Remote Sensing & GIS, Northwest German Forest Research Institute, Grätzelstr. 2, 37079 Göttingen, Germany

the most meaningful factors and describing their effect on tree damage by storms in a plausible way. In their application, well-parameterised models are able to generalise these effects to new settings by robust predictions of storm damage vulnerability for forest stands at different locations in different climatic conditions.

Forest storm damage models generally follow a mechanistic or a statistical approach. Mechanistic models aim to describe the physical properties of a wind-tree system. In particular, they describe how effective forces and the reactions of trees result in either windthrow or stem breakage. Mechanistic models allow a close representation of the cause-effect-relationship of tree damage, but require substantial parameterisation effort for specific tree species in a region of interest. For example, a prominent mechanistic model *ForestGALES* (Gardiner et al. 2000) is parameterised for forests of Great Britain (Hale et al. 2015), Finland (Peltola et al. 1999), or Canada (Byrne and Mitchell 2012). Its application is restricted to a few stands in Germany with comparable species composition and growth conditions. An alternative approach, statistical storm damage modelling, is based on empirical data typically derived from forest inventories and remote sensing. It relates the observed outcome (e.g. a binary variable tree undamaged / damaged) to a set of explanatory variables by the statistical properties of the data. The most prominent algorithms for statistical storm damage modelling were, for example, logistic regression (Schmidt et al. 2010; Kamimura et al. 2016; Suvanto et al. 2019) and machine learning classification techniques (Hart et al. 2019; Albrecht et al. 2019; Suvanto et al. 2019). Statistical models perform well within the range of their training data. Hence, a large data basis that covers wide gradients of all important factors generally leads to more robust effect estimates and to a better generalisation.

For their application, models ideally contain predictors, which are either directly or indirectly affected by management decisions. This allows for linking management options with damage probabilities (i.e. vulnerabilities) and, hence, supports forestry decision making. Common predictors in statistical storm damage models were derived from features of individual trees, stands, site, and orography (Hanewinkel et al. 2010). Schmidt et al. (2010) showed plausible and meaningful effects for tree species, dendrometric variables, soil water regime and topographic exposition with respect to the main wind direction. In this way, management options such as the choice of site-adapted tree species and target diameter can be attributed to storm damage probabilities. Nevertheless, wind speed as a predictor for storm damage in forest, is less frequently found in statistical modelling. Gusts, in particular, are the direct physical forces effecting tree crowns and leading to their drag, bending, swaying, and, in the end, to stem breakage or uprooting. Due to the mechanistic nature of this interaction, gust speed has commonly

been included in mechanistic models (Gardiner et al. 2008; Kamimura et al. 2016). Statistical storm damage models that can be used for robust predictions usually cover large areas and, hence, a continuous spatial representation of gust speed is needed for their parameterisation and application.

For storm damage modelling, gust speed fields must be spatially highly resolved ($< 100\text{ m} \times 100\text{ m}$), accurate, and temporally explicit. However, these properties are not present in the commonly available gust speed data. The wind speed measurement network of weather services is much too sparse and thus does not represent the high variability of gust speed. The rather coarse spatial resolution of reanalysis models (e.g. $0.25^\circ \times 0.25^\circ$ for ERA5 (Muñoz-Sabater et al. 2021)) is also unsuitable for statistical storm damage modelling. Besides, it is problematic to use mean wind speed from wind atlases as a predictor because each damage-inducing storm has its specific storm track. Due to these shortcomings, Jung and Schindler (2019) developed a winter storm atlas of the most severe winter storms in Germany from 1981 to 2018 (GeWiSa). GeWiSa includes highly resolved ($25\text{ m} \times 25\text{ m}$) maximum gust speeds for the 98 most severe storms.

In the absence of an explicit representation of gust speed, Schmidt et al. (2010) used a spatially structured effect (Brezger and Lang 2006) in the predictor set to model local tree damage emergence. This proxy variable most likely describes the spatially autocorrelated gust speed among other, unobserved factors. More recent studies use fine resolution gust speed fields to employ the direct agent in storm damage models. For example, Albrecht et al. (2019) showed moderate to good validation results for models with storm event-specific gust speed data as the only predictor (for single tree damages after storm events Vivian/ Wiebke 1990 and Lothar 1999 in Southwest Germany). However, when modelled together with a set of other dendrometry- and topography-related predictors, the additional gust speed effect did not improve the model considerably. For Finland, Suvanto et al. (2019) used high-resolution spatial data describing the long-term wind regime to model forest stand damage. Although they used rather general 10-year return-rates of gust speeds for parameterisation, the variable showed a significant contribution with a moderate sensitivity.

Statistical storm damage models usually make use of observations either at stand (Suvanto et al. 2019) or at individual tree level (Schmidt et al. 2010; Albrecht et al. 2019). Stand-level approaches average dendrometric variables like tree height, typically derived from forest inventories, at the cost of information loss. Single-tree models, in turn, need to take into account that observations from a forest inventory plot are not independent from each other. Multi-level models account for such structure in data and allow for the quantification of inter-group variation (Gelman and Hill 2007).

This variation includes information about storm damage at group level, for instance damage propagation to neighbours, which is usually either neglected or set aside but rarely used to inform predictions with statistical models.

In this study, we present a statistical approach to assess winter storm vulnerability of forests by modelling damage probabilities of single trees. The motivation was to achieve a high degree of generalisation for applications like decision support systems. For this, a large data set of one of Central Europe's most important storm events of the last decades was used. A focus was set on the explicit integration of a fine-grained spatial representation of near-surface gust speed as the direct driver for damage occurrence.

Materials and methods

Storm damage data

On December 26th, 1999 winter storm Lothar severely affected large parts of East France, Switzerland, and South-West Germany with maximum gust speed exceeding 50 m s^{-1} (Jung and Schindler 2019; Wernli et al. 2002). Shortly afterwards, Germany's second National Forest Inventory started and was completed in 2002. We used a spatial subset of this inventory data covering the federal state of Baden-Württemberg, the most important forest damage hot spot of Lothar in South-West Germany (Fig. 1B). The nested systematic sampling took place at locations (tracts) arranged on a $2 \text{ km} \times 2 \text{ km}$ grid, each with one to four nested sampling

sites (tract corners) arranged on a square with 150 m side length. All tract corners within a forest patch were sampled. Twelve tracts were excluded from the analyses because no gust speed information was available. In total, the data set included 63 117 trees (6613 damaged) on 11 000 tract corners organized in 4223 tracts. Measurements followed the standard German National Forest Inventory protocol (Kändler 2009) with a special record in Baden-Württemberg for individual trees damaged. Tree damage definition included wind throw and stem breakage. This binary variable (no damage or damage) per individual tree served as the response variable in our study.

For validation of these models, we processed a second inventory data set. In order to test the ability of the models to generalise, it was chosen to be spatially and temporally independent from storm event Lothar in South-West Germany. On January 18th, 2018 winter storm Friederike hit Great Britain, North France, the Netherlands, Belgium, and Germany. Although its maximum gust speeds were not as extreme as Lothar's, Friederike led to severe forest damage with a regional focus on the federal states of North Rhine-Westphalia, Lower Saxony, and Hesse in Central Germany (Jung and Schindler 2019). Contrary to the storm event Lothar, no inventory of trees damaged by Friederike was undertaken. Therefore, we assessed storm damage for a region in southern Lower Saxony (Fig. 1C) by interpretation of aerial ortho-photography. Aerial imagery from a flight survey conducted a few weeks after the storm event on February 6 and 13, 2018, was used. The flight survey covered in total 315 000 ha containing a forest area of 120 000 ha. Based

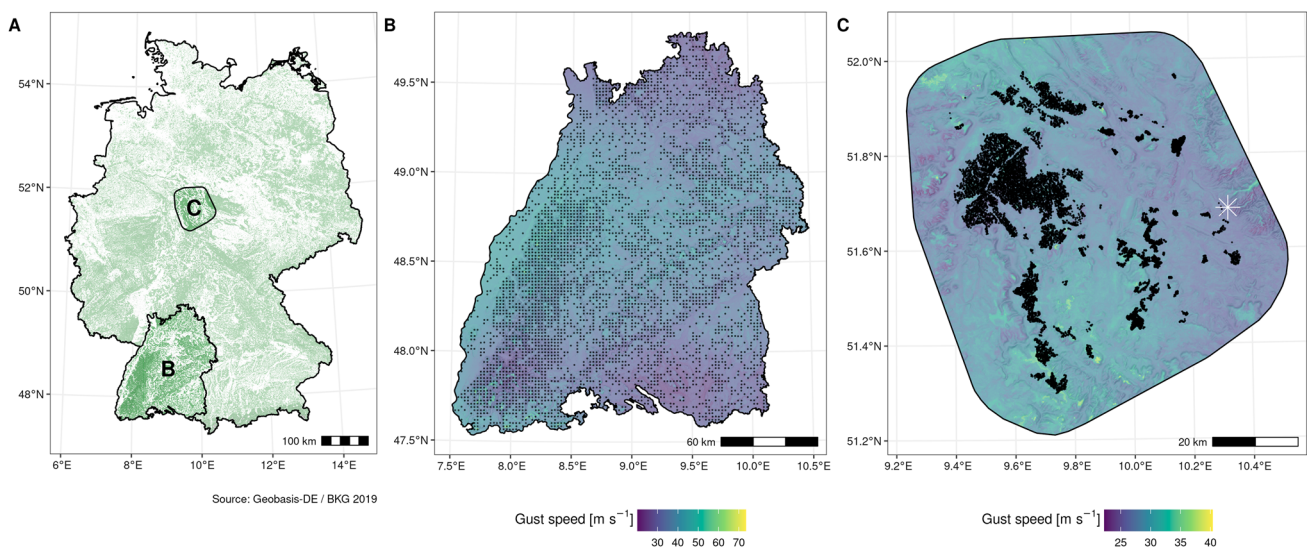


Fig. 1 A Forest distribution across Germany and the locations of the study areas. B Federal state of Baden-Württemberg with dots marking the tract locations of the national forest inventory. Colored background show maximum gust speed for storm event Lothar 1999. C Study region and inventory plots for model validation in South Lower

Saxony with gust speed for storm event Friederike 2018. The white asterisk at the eastern margin marks the site, of which the climatic and edaphic conditions were used to model dendrometric variables for sensitivity analysis. (Colour figure online)

on digital color-infrared ortho-photos, all forest patches with a coverage of at least 70% damaged crown surface and with a minimum area of 0.2 ha were delineated manually by visual interpretation. A minimum area of 0.2 ha was chosen a) to reduce the delineation error due to shadow casting, and b) to limit the total mapping effort. Reference ortho-photography from 2016 was compared in order to exclude areas which had been damaged and/ or cleared before storm event Friederike. To obtain stand damage data for validation, we processed forest sample plot data at enterprise level from the federal forestry administration Niedersächsische Landesforsten and intersected plot locations with damage polygons. This data set encompassed surveys on a total of 10 900 plots of which 374 intersected with delineated storm damage polygons.

Predictors

The set of predictor variables was taken from the predecessor model described in Schmidt et al. (2010). No further variable selection was performed to ensure comparability.

Tree features with an impact on wind-stress mechanics were included in the model. These were tree species and two dendrometric variables: tree height (*height*) and diameter at breast height (*dbh*). Tree species were grouped according to Schmidt et al. (2010): *Picea abies* (L.) H. Karst., *Fagus sylvatica* L. and *Quercus sp.* L., *Abies alba* Mill. and *Pseudotsuga menziesii* (Mirbel) Franco, *Pinus sylvestris* L. and *Larix decidua* Mill., and other deciduous species. Dendrometric variables at the time of the storm event needed to be estimated by single tree growth models. In the case of event Lothar, *height* and *dbh* values were taken from Schmidt et al. (2010). Based on a complete record of all *height* and *dbh* measurements from the first National Forest Inventory in 1987, they predicted *height* and *dbh* for 1999 with a fully initialized single tree growth model. For the values of the dendrometric variables at event Friederike, we processed forest sample plot data at enterprise level from the federal forestry administration Niedersächsische Landesforsten. The repeated surveys took place in the years 1991–2019. At each plot, *dbh* was measured for trees within two concentric circles with a radius of 6 m for individuals i with $7 \text{ cm} \leq \text{dbh}_i < 30 \text{ cm}$, and 13 m for $\text{dbh}_i \geq 30 \text{ cm}$ (Sabrowski et al. 2010). *height* was measured for one representative individual per plot, survey, and species. To obtain *height* and *dbh* at the time of storm event Friederike 2018, we first fitted for each tree species a linear mixed model with response variable *dbh*, variables *age* and *stand layer* as predictors, and *plot id* as group level. These models were used to predict *dbh* in 2018 for each tree. Then, mean quadratic diameter (*mqd*) in 2018 was calculated per species and plot. Finally, corresponding tree heights, h_{mqd} were predicted by height-diameter curves calibrated with the *height*-*dbh*-pairs

of representative trees (Lappi 1997; Schmidt 2009). These means of the dendrometric variables were used since damage information was available at plot level only.

Gust speed is supposed to be an important driving force for storm damage on trees. Based on empirical data and orographic features, Jung and Schindler (2019) developed the high-resolution gust speed atlas GeWiSA for 98 severe winter storms in Germany in the period 1981–2018. This data was used to obtain the predictor maximum gust speed (*gs*). The metric is defined as the maximal wind speed lasting for at least 3 s at a height of 10 m during a storm event.

The topographic situation of a site was depicted by a distance-based topographic exposure index (*topex*) (Scott and Mitchell 2005). It quantifies the aspect and degree of exposure for each site by measuring the angle to the horizon for a given bearing and distance. Exposed sites show negative *topex* values, plains have values around zero, and sheltered sites are characterised by positive *topex* values.

We summed up *topex* values of two bearings spanning a given angle around the main storm wind direction. This ensures an identical effect of topography for both deviations from the main wind direction. Distance and angle choice followed the model selection of Schmidt et al. (2010). In total, we calculated three *topex* sums for a distance of 1000 m: 1) pointing in the main direction of the storm (*topex upwind*) with bearings spanning an angle of 30°, 2) pointing away from the main storm direction (*topex downwind*) with bearings spanning a 30° angle, and 3) pointing orthogonal to the main storm wind direction (*topex crosswind*) with 180° between bearings. The latter replaced two wide-angled *topex* sums used by Schmidt et al. (2010), which were auto-correlated. The three pairs of *topex* sums are suited for a comprehensive description of orography with sensitivity to an assumed wind direction. *Topex upwind* sums describe exposed and sheltered locations. In combination with *topex downwind* sums, topographic elements like slopes, saddles, and ridges perpendicular to the main wind direction are distinguished. *Topex crosswind* sums accentuate ridges and valley floors in the direction of the storm. All *topex* sums were calculated on basis of the Copernicus Digital Elevation Model Cop-DEM-GLO90 (Release 2020) (Copernicus 2020).

Information on soil water characteristics was included as a proxy for different rooting zone conditions and, hence, the ability of a tree to anchor in the soil. This variable was derived from the water regime category of the forest site mappings for Baden-Württemberg and Lower Saxony. Forest site mapping assesses pedological, geomorphological, hydromorphological, and geobotanical features of site and soil. In Germany, forest site mapping of the federal states varies in methodology and units, and, hence, the level of detail. In the parameterisation, data from Baden-Württemberg soil water regime was categorized in 28 units grouped

in three classes: terrestrial, ground-water influenced, and waterlogged. In order to reduce the number of parameters we pooled these 28 units into storm-specific categories by effect comparison and expert knowledge. In Lower Saxony soil mapping units encompassed a total number of 43 major water categories differentiated into up to three subcategories. These units were manually reassessed and attributed to the pooled storm-specific groups.

Modelling

We followed two different approaches for modelling damage by storm event Lothar using the training data. The first, *SSE*, was a generalised additive model (Bernoulli distributed, logit link-function) with a spatially structured effect as described in Schmidt et al. (2010). It was fitted as a benchmark model which did not include any explicit gust speed information. For each tree individual i , the binary response

$$y_i = I_{\text{tree } i \text{ damaged}} \tag{1}$$

after storm event Lothar, where

$$I_{\text{condition}} = \begin{cases} 1, & \text{if condition is true,} \\ 0, & \text{else.} \end{cases} \tag{2}$$

is a binary indicator, was modelled by a logistic regression as follows:

$$\begin{aligned} y_i &\sim \text{Bernoulli}(p_i) \\ p_i &= \frac{\exp(\eta_i)}{1 + \exp(\eta_i)} \quad (\text{logit link-function}) \\ \eta_i &= \mathbf{x}_i^\top \boldsymbol{\beta} + f(\text{east}_i, \text{north}_i) \end{aligned} \tag{3}$$

Damage probability p_i as the only parameter of a Bernoulli random variable was modeled by a set of individual-specific covariates \mathbf{x}_i and its respective regression parameters $\boldsymbol{\beta}$. The covariates were: tree species, log (height), and log (dbh) in interaction with tree species, soil water category, and the three topex sums, namely upwind, downwind, and crosswind. There was no valid information about wind speed available for Schmidt et al. (2010) so that it was necessary to assume spatial location to be a valid proxy for maximum gust speed, gs_i . For that $f(\text{east}_i, \text{north}_i)$, a two-dimensional, isotropic smoothing spline over the spatial coordinates was included in a Generalized Additive Model framework (Wood 2017). Further, no group effects for tracts and tract corners could be estimated because of strong confounding with the two-dimensional spatial trend function. Refitting was necessary because of minor changes in the data basis as well as in the predictor set. First, information on site soilwater regime was updated. Further, we detected a considerably high correlation between two different topex

sums spanning a wide angle around the main wind direction. Consequently, we replaced them with one crosswind topex sum.

In a second, multilevel approach we accounted for the inventory design by which tree individual i is nested in tract j and tract corner k . We therefore included group intercepts

$$u_i = \sum_{j=1}^J I_{\text{tract},=j} u_j \tag{4}$$

for tracts, and

$$v_i = \sum_{j=1}^J \sum_{k=1}^4 I_{\text{tract},=j \text{ and corner},=k} v_{j,k} \tag{5}$$

for tract corners:

$$\begin{aligned} y_i &\sim \text{Bernoulli}(p_i), & p_i &= \frac{\exp(\eta_i)}{1 + \exp(\eta_i)}, \\ \eta_i &= \mathbf{x}_i^\top \boldsymbol{\beta} + u_i + v_i, \\ u_j &\sim \text{Normal}(0, \sigma_u^2), \\ v_{j,k} &\sim \text{Normal}(0, \sigma_v^2). \end{aligned} \tag{6}$$

Here, we tested two different strategies for replacing the spatial smoothing function of *SSE* by the predictor gs . In a parametric model, *PGS*, we assumed an exponential effect of gs on the response. In this scenario we added gs^2 to \mathbf{x} . By fixing the exponent to the value 2 here, we followed the rationale of fluid mechanics where the drag force affecting a given area (i.e. tree crown) is proportional to the squared velocity (i.e. gust speed) (Moore et al. 2018).

The second approach for replacing the spatial smoothing function is to include the effect of gs as a smoothing spline within a Generalized Additive Mixed model framework (*SGS*). Here, the effect of gs on tree damage is modelled by a thin-plate regression spline (Wood 2017). This flexible framework allows for the selection of the most plausible functional relationship between gs and storm damage probability, based on information from the data only, and not by any domain expertise as utilized in the first strategy. In order to elucidate the importance of gs as a predictor, *PGS* and *SGS* were compared against a reference model (*NGS*) which included all predictors but not gs .

All model formulation and fitting was conducted within a Bayesian framework. Continuous covariates were centered by their arithmetic mean and scaled to the unit of one empirical standard deviation. We used $\text{Normal}(0, \sigma = 5)$ as a weakly informative prior distribution (Lemoine 2019) for every population-level parameter in $\boldsymbol{\beta}$. The estimation of variances σ_u^2 , and σ_v^2 for group level parameters was based

on a half Student-t prior with 3 degrees of freedom and a scale of 5.

Models were estimated by launching four parallel Markov chains of 2000 iterations from which the first 1000 steps were discarded as *warm-up*. After model fitting chain convergence was assured by checking the *Gelman and Rubin convergence diagnostic* \hat{R} to be less than 1.01 and the effective sample size being greater than 1000 (Gelman et al. 2013).

Predicting with multi-level models for data not belonging to the National Forest Inventory of Baden-Württemberg faces the problem that group membership (in our case tract and tract corner groups) is unknown. One possible option, marginal predictions with group-level effects set to 0, was shown to lead to poorer predictive performance (Skrondal and Rabe-Hesketh 2009; Pavlou et al. 2015). Therefore, we fitted a mixture distribution model with the combination of estimated tract and tract corner effects on a logit scale. We drew 1000 samples from this mixture distribution, added each to the linear predictor combination, and calculated damage probability by inverting the logit scale and taking the mean. This resulted in a marginal prediction informed by group level effects. A similar problem arises when predicting with *SSE*: the spatial smoothing function is parameterised with coordinates of Baden-Württemberg. When predicting storm damage probability outside this spatial domain for South Lower Saxony, we projected averaged conditions of storm event Lothar onto the model estimates. Therefore, we sampled the spatial effects of 1000 tract coordinates of the parameterisation data set. Each of those were added to the linear predictor combination and transformed to damage probability by the inverse logit function. Finally, the mean of the resulting 1000 probability values was used.

Validation

Sensitivity analyses of predictor effects were performed by using a time series of dendrometric variables estimates for a simulated forest stand at an exemplary location at the western margin of the Harz mountains, Germany (Fig. 1C). The simulated forest was represented by a mean stand tree for each species, of which h_{mqd} was calculated using a climate-sensitive site index model (Schmidt 2020) and mqd was predicted by a site-sensitive inverted longitudinal height-diameter curve (Schmidt 2009). This development of mqd and h_{mqd} over time was calculated for ages 30–130 (30–150 for *Quercus sp.* + *F. sylvatica*) in time steps of 10 years. The year of germination of these mean stand trees was set to 1950. Beginning with 2020, climate input data was retrieved from a subset of EURO-CORDEX ensemble containing seven representative projections (ReKliEs-De; Warrach-Sagi et al. (2018)) for scenario RCP 8.5. For each

time step and age respectively, the corresponding h_{mqd} and mqd values were averaged over these projections.

Predictive performance was tested by two approaches. First, all models were compared by a 20-fold cross validation with the parameterisation data set of Lothar. Data were split by keeping all observations of the same tract together. This ensured independence between training and test data. Two measures for predictive performance were used for validation: expected log pointwise predictive density (*elpd*) (Vehtari et al. 2017) and area under receiver-operator characteristics curve (*AUC*). *Elpd* is a measure for out-of sample predictive accuracy, which uses within-sample fits with higher values for better performance. *AUC* is a common classification metric which relates the true positive rate to the false positive rate for binary predictions at different probability thresholds. For model comparison, *AUC Lothar* was averaged over the 20 cross validation runs and *AUC Friederike* was calculated with the independent validation data for Friederike in Lower Saxony.

All data analyses and plotting were done in the statistical programming environment *R* (R Core Team 2021). Fitting and cross-validation of models was realized with *brms* (Bürkner 2017, 2018), which is based on *Stan* (Carpenter et al. 2017). *AUC* calculation was done with *pROC* (Robin et al. 2011).

Results

Model fits showed significant effects for most predictors, 95% credible intervals did not include a value of 0 (Table 1). Exceptions were the interaction between tree species *other deciduous species* with dbh as well as two soil water category: *groundwater-influenced* and *terrestrial*. Storm damage models *SSE*, *PGS*, and *SGS* showed same effect directions for covariates they shared, with smaller amplitudes for *SSE* than for *PGS* and *SGS*, especially for the dendrometric variables. In general, covariate effects of *PGS* and *SGS* differed only slightly.

Figure 2 A allows for effect comparison of the two different approaches to model gs. The non-linear effect of *SGS* showed the strongest monotonic increasing effect in a gs range from 31 to 46 m s⁻¹ where it increased by 5 units on the logit scale. At values above 46 m s⁻¹ effect variation was very high and its average was decreasing with higher speeds due to lower data density. *PGS* constrained the effect of gs to a quadratic relationship. The effect increased monotonically and in total it spanned a large amplitude of more than 10 units on the logit scale. This large amplitude resulted in a steep increase of corresponding damage probabilities (Fig. 2 B). At top gs between 50 m s⁻¹ and 60 m s⁻¹, damage probabilities predicted by *PGS* increased from 0.2 to more than 0.85. This is in contrast to estimates from *SGS*, whose upper

Table 1 Coefficient estimates of different model variants (columns), that were: a spatially structured effect (SSE), a parametric representation including squared gust speed (PGS), a spline function of gust speed (SGS), and excluding the parameter gust speed (NGS)

Predictors	Estimates (CI 95%)							
	SSE		PGS		SGS		NGS	
Tree:								
<i>P. abies</i>	-2.33	(-2.40, -2.24)	-6.17	(-6.53, -5.83)	-6.18	(-6.56, -5.82)	-6.61	(-6.99, -6.24)
<i>A. alba</i> + <i>P. menziesii</i>	-2.76	(-2.88, -2.64)	-6.80	(-7.21, -6.39)	-6.83	(-7.25, -6.41)	-7.15	(-7.58, -6.72)
<i>P. sylvatica</i> + <i>L. decidua</i>	-3.43	(-3.56, -3.30)	-7.61	(-8.05, -7.19)	-7.64	(-8.09, -7.21)	-8.03	(-8.47, -7.58)
<i>F. sylvatica</i> + <i>Quercus sp.</i>	-4.10	(-4.22, -3.99)	-8.51	(-8.94, -8.11)	-8.54	(-8.98, -8.13)	-8.91	(-9.34, -8.49)
Other deciduous species	-4.49	(-4.68, -4.30)	-8.44	(-8.96, -7.96)	-8.48	(-9.00, -7.99)	-8.73	(-9.24, -8.22)
<i>P. abies</i> :log(height)	1.24	(1.15, 1.33)	2.52	(2.30, 2.75)	2.52	(2.28, 2.76)	2.47	(2.24, 2.71)
<i>A. alba</i> + <i>P. menziesii</i> :log(height)	0.56	(0.41, 0.72)	1.67	(1.34, 2.02)	1.67	(1.33, 2.02)	1.62	(1.29, 1.96)
<i>P. sylvatica</i> + <i>L. decidua</i> :log(height)	0.96	(0.76, 1.16)	1.67	(1.31, 2.05)	1.67	(1.30, 2.04)	1.66	(1.29, 2.03)
<i>F. sylvatica</i> + <i>Quercus sp.</i> :log(height)	1.10	(0.95, 1.25)	1.80	(1.51, 2.10)	1.81	(1.51, 2.12)	1.79	(1.50, 2.09)
Other deciduous species:log(height)	0.53	(0.31, 0.77)	1.16	(0.78, 1.56)	1.15	(0.76, 1.56)	1.16	(0.76, 1.56)
<i>P. abies</i> :log(dbh)	-0.60	(-0.69, -0.52)	-1.34	(-1.52, -1.15)	-1.34	(-1.52, -1.15)	-1.29	(-1.48, -1.10)
<i>A. alba</i> + <i>P. menziesii</i> :log(dbh)	-0.15	(-0.29, -0.01)	-0.77	(-1.03, -0.50)	-0.77	(-1.02, -0.52)	-0.75	(-1.01, -0.48)
<i>P. sylvatica</i> + <i>L. decidua</i> :log(dbh)	-0.64	(-0.84, -0.44)	-0.95	(-1.30, -0.60)	-0.95	(-1.31, -0.58)	-0.93	(-1.29, -0.56)
<i>F. sylvatica</i> + <i>Quercus sp.</i> :log(dbh)	-0.40	(-0.51, -0.29)	-0.64	(-0.85, -0.43)	-0.65	(-0.86, -0.43)	-0.62	(-0.83, -0.40)
Other deciduous species:log(dbh)	-0.12	(-0.33, 0.08)	-0.08	(-0.42, 0.27)	-0.07	(-0.43, 0.26)	-0.03	(-0.04, 0.33)
Site:								
Soil water regime:Groundwater-influenced	-0.14	(-0.37, 0.10)	0.36	(-0.64, 1.30)	0.31	(-0.73, 1.29)	0.95	(-0.09, 1.92)
Soil water regime:Waterlogged	0.63	(0.51, 0.75)	1.30	(0.74, 1.85)	1.30	(0.72, 1.87)	1.57	(0.99, 2.17)
Soil water regime:Shallow terrestrial	0.42	(0.30, 0.52)	1.01	(0.52, 1.49)	0.99	(0.51, 1.49)	1.54	(1.03, 2.03)
Soil water regime:Terrestrial	-0.07	(-0.15, 0.01)	0.15	(-0.19, 0.50)	0.13	(-0.24, 0.49)	0.67	(0.31, 1.03)
Topex upwind	-0.51	(-0.55, -0.47)	-0.91	(-1.12, -0.72)	-0.93	(-1.14, -0.74)	-1.07	(-1.27, -0.85)
Topex downwind	-0.26	(-0.30, -0.21)	-0.54	(-0.74, -0.34)	-0.54	(-0.75, -0.33)	-0.57	(-0.79, -0.36)
Topex crosswind	0.28	(0.24, 0.32)	0.65	(0.45, 0.84)	0.65	(0.45, 0.86)	0.65	(0.44, 0.85)
Gust speed:								
gs ²			1.33	(1.17, 1.50)				
σ s(gs) (df = 2)					8.33	(3.05, 18.33)		
Group effects:								
σ u (n = 4223)			3.02	(2.81, 3.24)	3.00	(2.78, 3.22)	3.37	(3.14, 3.60)
σ v (n = 11 000)			3.31	(3.13, 3.49)	3.33	(3.14, 3.51)	3.31	(3.14, 3.49)
Spatial effect:								
σ s(east,north) (df = 197)	12.15	(10.72, 13.74)						

Values are means of the posterior distribution and their 95% credible interval (CI). If CI includes 0 figures are set in italics. Estimates for smoothing splines are given as variance components with 0 for a straight line and the higher its values the higher the degree of wiggleness. Degree of freedom (df) defines the number of estimated parameters

bound of the 0.95 credible interval was less than half of the level of PGS. In the same gs range, the posterior mean of SGS was with less than 0.15 very low and even decreased with higher gs values.

Combining the effects of tree species and its interactions with tree height and dbh in PGS, *P. abies* showed

the highest absolut storm damage probabilities (Fig. 3), followed by the species groups *A. alba* + *P. menziesii*, *P. sylvestris* + *L. decidua* and *Quercus sp.* + *F. sylvatica*. With gs = 30 m s⁻¹, all species have similar damage probabilities at height = 15 m. With tree height = 30 m, *P. abies* showed a relative damage probability 1.5 times

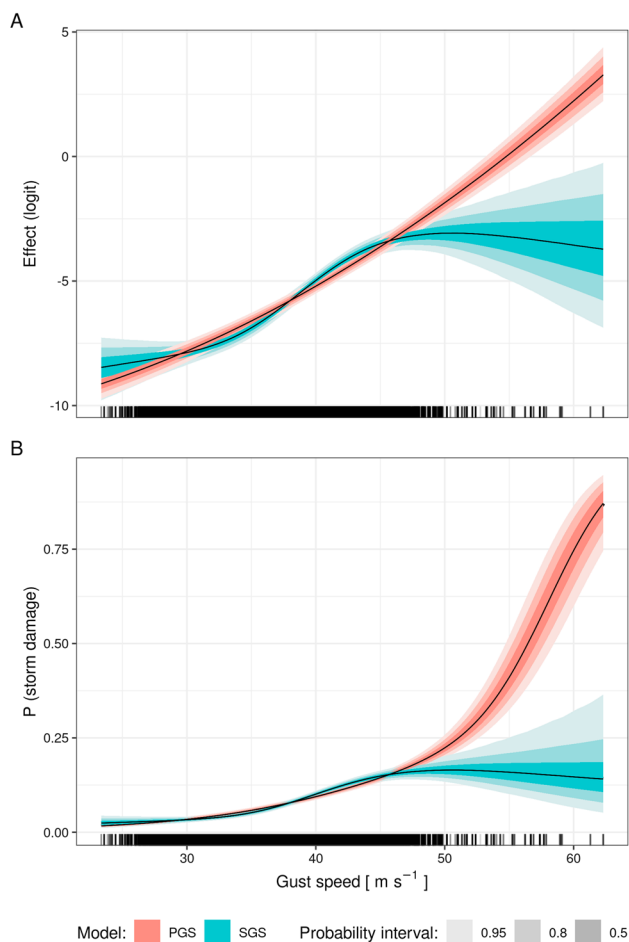


Fig. 2 Conditional effect of gust speed (gs) of two different approaches to model storm damage probability. *SGS* used a spline function for *gs* and *PGS* included squared *gs* as a linear covariable. The effect is displayed **A** on the scale of the predictor term and **B** transformed to storm damage probability. Black lines and different shading intensities show median and quantiles of the posterior distribution. All other metric predictors were set to their mean. Categorical predictors were set to tree species *Picea abies* and soil water category *terrestrial*. Ticks on the x-axis mark *gs* values of the parameterisation data. (Colour figure online)

higher than *A. alba* + *P. menziesii*, 2 times higher than *P. sylvestris* + *L. decidua*, and 3 times higher than *Quercus sp.* + *F. sylvatica*. With increasing *gs*, *P. abies* still showed the highest damage probabilities, but the relative difference to other species decreased. For instance, at height = 30 m the damage probability of *P. abies* was 3 times higher than *F. sylvatica* with $gs = 30 \text{ m s}^{-1}$, but 2 times higher with height = 50 m. Slight differences within tree species groups were caused by species-specific estimations of the dendrometric variables and hence, height-to-diameter ratios. This difference was most pronounced for *Quercus sp.* + *F. sylvatica* over all heights, but also *P. menziesii* + *P. abies* differed slightly at heights > 35 m and *P. sylvatica* + *L. decidua* at heights > 30 m

Storm damage showed the highest sensitivities for topex sums in upwind and crosswind directions (Fig. 4). Negative upwind topex sums indicated storm-exposed sites with the highest damage probabilities. Sheltered sites had positive topex sums and the lowest vulnerabilities. Negative crosswind topex sums described topographic ridges stretching in the wind direction and were associated with low storm damage risk. Positive crosswind topex sums indicated locations in narrow valley bottoms stretching in the wind direction. Here, high storm damage probabilities were associated, as a result of a tube-effect, with higher expected wind speed. Among all three topex sums, the downwind variant showed the weakest effect amplitude.

Pooling of soil water mapping units resulted in four storm-specific categories: *terrestrial*, *shallow terrestrial*, *groundwater-influenced*, and *waterlogged* soils. Comparing the sensitivity to these categories, periodical *waterlogged* soils and *shallow terrestrial* soils showed higher damage probabilities than *terrestrial* and *groundwater-influenced* soils (Fig. 5). Low probabilities for soil water category *terrestrial* and *groundwater-influenced* were a result of effect sizes close to zero (Table 1).

Both group effects on tract and on tract corner level, as well as their combination, showed a bimodal distribution pattern (Fig. 6A–C): a slightly negative mode with low variation and a distinctly positive mode with large variation. This empirical distribution was fitted by a mixture model of two distributions (see supplementary information S11): a Normal(−1.4, 0.9) and a Student’s *t* distribution with $\nu = 77$ (degrees of freedom), $\mu = 3.23$ (location), and $\sigma = 3.57$ (shape). The mixture weight for the normal distribution was 0.7. The empirical density distribution of combined group level estimates could be approximated by 1000 samples of the mixture distribution (Fig. 6C).

Out-of-sample 20-fold cross validation using *elpd* showed that model *SSE* performed best (Table 2). By including *gs* as a predictor, *PGS* and *SGS* showed better results than model *NGS*. A similar picture provided the ranking of models by *AUC* values. In contrast, predictive performance with independent data from storm event Friederike did not differ between models *PGS* and *SGS* but showed a higher *AUC* value for *NGS*. Again, *SSE* showed best performance here.

Discussion

The multi-level modelling approach presented here integrates a) site-related factors like orography and soil features, b) species-specific dendrometric characteristics, and c) near-surface gust speed information to estimate a single tree storm damage probability. This probability provides a comprehensive assessment of forest vulnerability to winter storm damage. By replacing the spatially structured effect

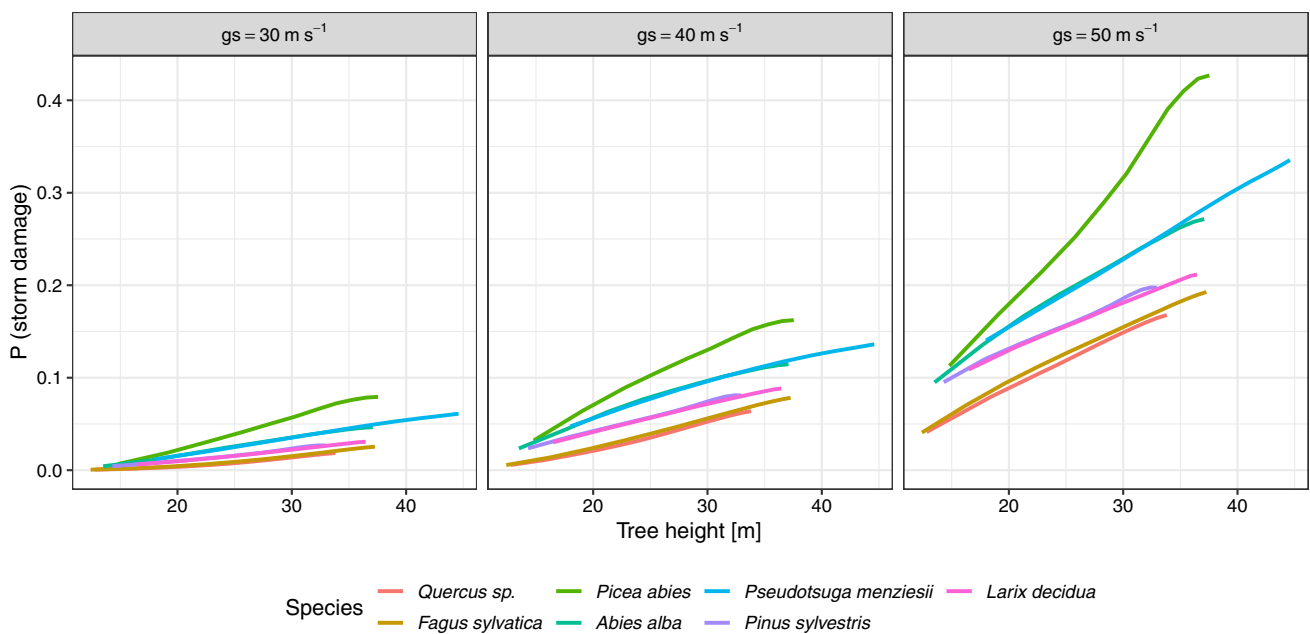


Fig. 3 Sensitivity of storm damage probability on tree height, species groups, and three different gust speeds (gs) from model PGS. Tree diameter at breast height (dbh) and height are predictions for mean quadratic diameter (mqd) and corresponding height (h_{mqd}) by climate-sensitive site index- and height-diameter-models at an

exemplary location on the eastern margin of the study area in Lower Saxony (322 m a.s.l), Germany Fig. 1C). All topex-to-distance sums were set to 0 (plain topography) and soil water category was set to *terrestrial*. (Colour figure online)

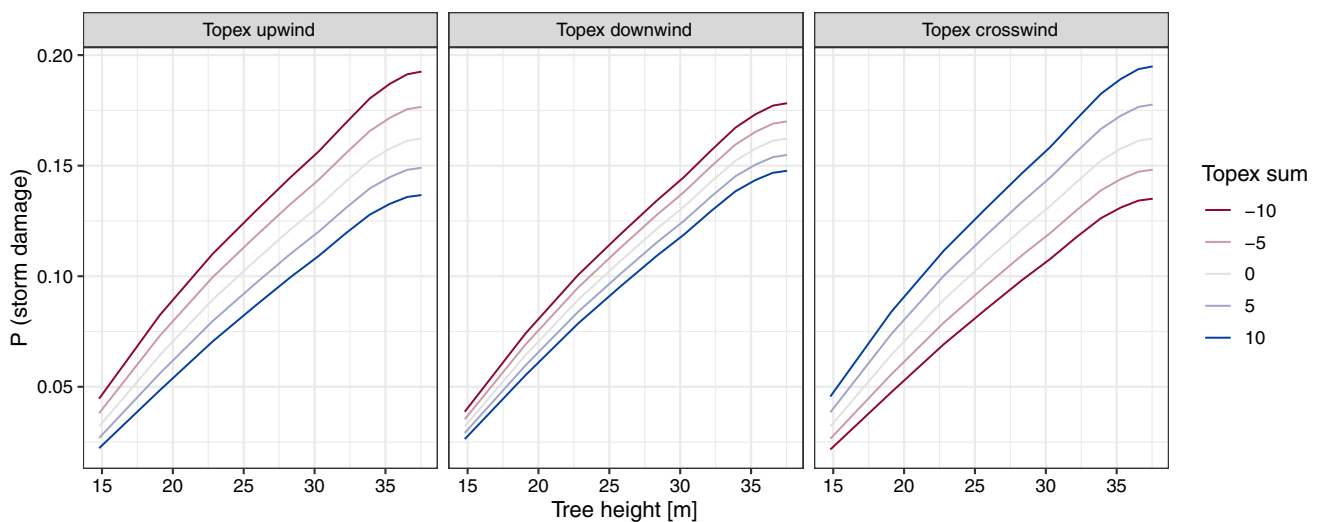


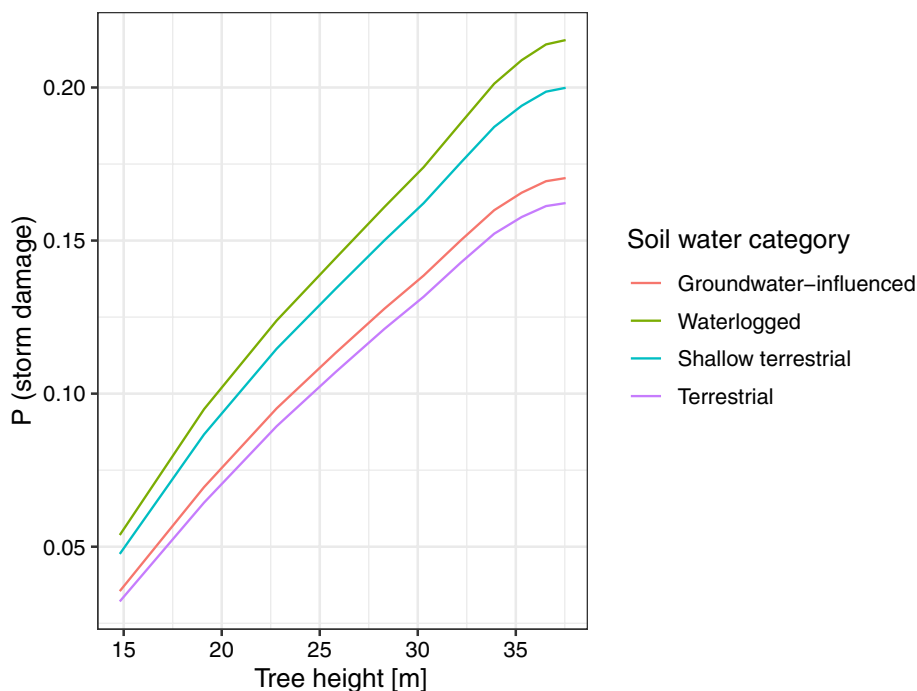
Fig. 4 Sensitivity of storm damage probability on three different topex-to-distance sum effects from model PGS on storm damage probability over different tree heights. Effects were calculated for the species *P. abies* with the same height and dbh estimates as in Fig. 3.

The remaining topex-to-distance sums were set to 0, gs was assumed to be 40 m s⁻¹ and soil water category was set to *terrestrial*. (Colour figure online)

of SSE with gs in PGS and SGS, we included direct spatial information on the driver of tree damage in the model. By modelling this direct agent for storm damage, we aimed for a high degree of generalisation in the model. However, in our validation results SSE outperformed both models with gs as

a predictor. The spatially structured effect of SSE accounts for autocorrelated heterogeneity on a regional scale (Brezger and Lang 2006). gs as a direct driver for storm damage most likely dominates this structured effect but it remains unclear to what extent and what other unobserved features have an

Fig. 5 Sensitivities of soil water category effects from model *PGS* on storm damage probability over tree height. Effects were calculated for the species *P. abies* with the same height and dbh estimates as in Fig. 3. All topex-to-distance sums were set to 0 and g_s was 40 m s^{-1} . (Colour figure online)



additional impact. The spatially structured effect, in turn, could interfere with spatially dependent covariates, which is known as spatial confounding (Clayton et al. 1993) and leads to biased effect estimates (Dupont et al. 2022). Indeed, we found less accentuated effect sizes in *SSE*. In contrast, the spatial predictor g_s and the hierarchical group effects of the approaches *PGS* and *SGS* clearly separate between wind-driven damage patterns and unmeasured local effects.

Comparing the different methods to implement g_s , a data-driven smoothing spline and a theory-based assumption of a quadratic relationship, the smoothing spline of *SGS* showed a diminishing effect at very high g_s . At exposed sites trees adapt to frequently windy conditions, for instance by thigmomorphogenesis (Bonnesoeur et al. 2016) or by a closer height-to-diameter ratio. The latter was modelled explicitly by the approaches presented here, but it is likely that the effect was confounded by a higher occurrence probability of trees with close height-to-diameter ratio at sites with top g_s . Further, it is possible that damaged trees are attributed with higher g_s than the actual value that lead to tree damage. The temporal aggregation of g_s to a maximum value over the passage of a storm event does not resolve the total duration, the frequency, or the sequence of gusts affecting the trees. For example, less extreme but repetitive g_s could also lead to swaying and subsequent stem-breakage (Brüchert and Gardiner 2006; Jackson et al. 2019), especially when trees are not adapted to such dynamics (e.g. inner stand individuals (Gardiner et al. 2016)). In contrast, *PGS* constrains the effect of g_s to an exponential increment, particularly at high g_s above 50 m s^{-1} . For the predictions it is more plausible

to project an increasing effect with higher g_s onto damage projections rather than dampening the effect because of possible tree adaptations. Although the g_s effect in *PGS* was superimposed by the quadratic relationship and, hence, was not as close to the data as compared to the spline of *SGS*, both models showed similar validation performance.

Even though g_s is the physical driver for storm damage, it did not improve prediction performance of *PGS* or *SGS* when validated with data from Friederike. Albrecht et al. (2019) reported similar findings. They modelled forest damages after two different storm events in Baden-Württemberg, Germany, and found a significant contribution of g_s for only one event Lothar, but not for the earlier winter storm Vivian/ Wiebke in 1990. Conditions such as soil frost or high soil water saturation can vary substantially between winter storm events, which in turn has an effect on the importance of g_s as a damage predictor. In the case of event Friederike, the storm had been preceded by a long period of rainfalls which resulted in high soil water saturation and a lowered root-soil anchorage. Here, tree species, height, and dbh would probably better explain damage occurrence than g_s nor soil water category.

Both multi-level models showed high sensitivities of damage probability for covariates related to tree dimension and slenderness in interaction with tree species. The ranking of species according to their storm damage susceptibility is consistent with the findings of the predecessor study by Schmidt et al. (2010) but also with several other studies as reviewed in Gardiner (2021). Especially *P. abies* and *A. alba*

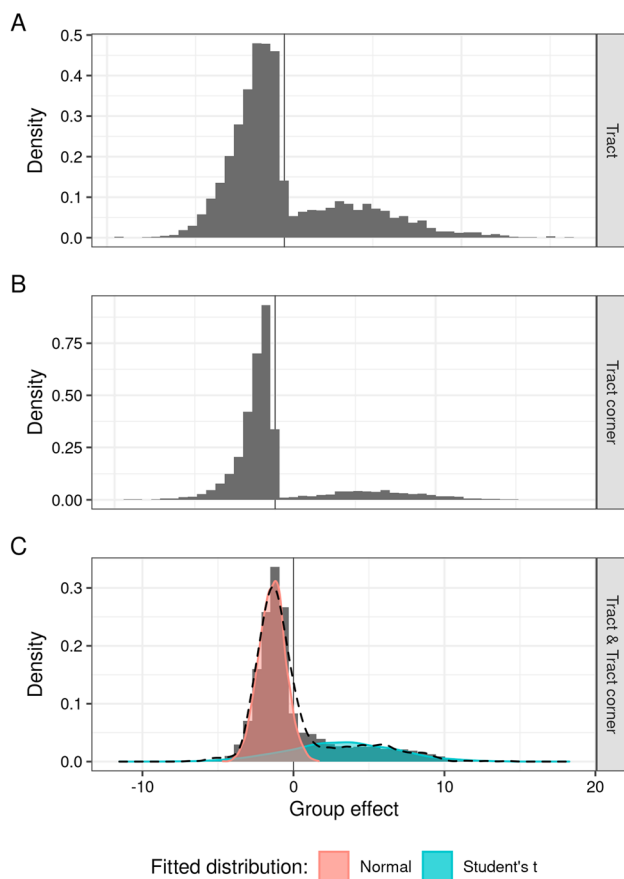


Fig. 6 Empirical density distributions as histograms of group level effects for tracts (A), tracts corners (B), and their sums (C) derived from model *PGS*. Group level effect sums (C) were approximated by a mixture model of two distributions: a Normal distribution (red) and a Student's *t* distribution (green). The dashed black line shows the density of 1000 samples drawn from this mixture distribution. (Colour figure online)

Table 2 Validation results for model variants: *SSE* spatially structured effect, *SGS* spline function of gust speed *gs*, *PGS* parametric model including squared *gs*, and *NGS* excluding *gs* as a covariate

Model	$\Delta elpd$	<i>AUC Lothar</i>	<i>AUC Friederike</i>
SSE	0.0	0.80	0.75
SGS	-863.1	0.77	0.71
PGS	-949.3	0.77	0.71
NGS	-1800.1	0.72	0.72

Statistic metrics *elpd* and *AUC Lothar* were derived from out-of-sample 20-fold cross validation of the parameterisation data of event Lothar. Values for *AUC Friederike* were calculated with predictions from Friederike storm data set for Lower Saxony

+ *P. menziesii*, economically important species, showed high vulnerabilities to winter storm damage. Their rapid height growth in relation to diameter increment leads to higher slenderness, i.e. wider height-to-diameter ratio. The crowns

of conifers form a larger surface area than those of deciduous species in the winter season. Additionally, the shallow root architecture of *P. abies* promotes a higher susceptibility to windthrow. Site-related effects of soil water categories and topex sums quantify the abiotic predisposition of a location. Positive coefficients of the soil categories *shallow terrestrial* and *waterlogged* underline the importance of limited anchoring due to shallow rooting zones. Although this should also apply to *groundwater-influenced* soils, the corresponding effect did not influence the damage probability. These soils are less common in low mountain range regions like Baden-Württemberg and they are typically restricted to less exposed valley floors. This might have had lead to confounding with e.g. topex crosswind. Additionally, it is possible that the effect differs substantially between tree species because of different root architectures. However, the data basis did not suffice to model tree species-specific effects of soil water category.

The combination of different topex sums relative to the main storm direction captures a large variety of orographic settings ranging from sheltered or exposed slopes to more complex forms, such as ridges or valley bottoms with different alignments. By step wise model selection, Schmidt et al. (2010) showed that these wind-direction sensitive topex sums better assess the orographic vulnerability to storms than the original topex, which sums up all eight (inter)cardinal directions (Scott and Mitchell 2005). Nevertheless, this implies for the assessment of possible damage vulnerabilities, that assumptions of the main storm directions have to be made. Most winter storms in Central Europe originate in the North Atlantic Oscillation and were driven by the westerlies, so that (south)west-orientated topex values are likely to depict the orographic exposure best.

Multi-level group effects of tracts and tract corners showed high variability compared to the effect sizes of the predictors. This variability integrates all regional and stand-level factors which have not been represented by the other predictors. The bimodal distribution of group level effects included a cluster of positive values. Here, more damage on tract or tract corner level occurred than was explained by the predictor set. Besides missing important measurable covariates, there are other causes which impact storm damage like stochasticity and damage propagation which are hard to quantify. In a storm event wind turbulence and resulting tree motion in combination with variation of individual tree features, such as rooting resistance, crown shape, or stem mechanics, lead to single tree failure and, due to damage propagation, to the loss of whole tree groups or stands (Dupont et al. 2015; Kamimura et al. 2019; Gardiner 2021). While simulations with mechanistic models (Dupont et al. 2015) and with agent based models (Kamimura et al. 2019) successfully emulated patterns of damage propagation, statistical models rarely used information from the stochastic

part in the prediction. In a different context, de Miguel et al. (2012) also found good performance for non-linear, multi-level taper models when using mean predictions over the distribution of group level effects. For predicting storm damage probabilities with stochastic information of the group level effects, the assumption is that the bimodal distribution found is rather a general winter storm related pattern than an event Lothar specific feature. However, climatic and environmental conditions, as well as the duration and intensity, differ between storm events and impact on the frequency and extent of tree damages. This inter-storm heterogeneity cannot be properly addressed because extensive data sets on damages caused by different events in a region of interest are missing. Nevertheless, the Lothar data set is extraordinary in terms of spatial coverage, number of observations, and covariate gradients covered, so it is most likely that the models depict main aspects of winter storm dynamics in Central Europe.

Conclusions

Winter storm damage probability was modelled in a comprehensive statistical framework based on a large data basis. This was accomplished by combining a deterministic part, including the most relevant features of dendrometry, soil water regime, orography, and a detailed spatial representation of gust speed, with a stochastic component describing unobserved variance at group level. Uncertainties about the origin of spatially correlated effects of its predecessor model *SSE* are replaced by the clear separation between information from the direct damage agent *gs* and stochastic variability in group effects. Due to the lower complexity and parametric formulation, the foundation in physical law, and the plausibility of the *gs* effect, *PGS* is most suitable for assessing storm damage vulnerability in forests. This framework is highly generalisable and allows for the assessment of winter storm vulnerability, for example, in the context of strategic forest planning. Further, the climate-sensitive predictors tree height, dbh, and *gs*, allow for the projection of vulnerabilities of actual or planned stands to future conditions (Jung and Schindler 2021). Within a forest enterprise, this information can be used to minimise storm damage risk by scheduling time of yield for present stands and optimising the spatial distribution of tree species for future stands.

Supplementary Information The online version contains supplementary material available at <https://doi.org/10.1007/s10342-023-01575-8>.

Acknowledgements This work was supported by the FNR (Fachagentur Nachwachsende Rohstoffe e.V.) within the framework of the Forest and Climate Fund (MiStriKli 22W-K-4-166-02). We would like to thank Heike Puhlmann (FVA-BW) for contributing soil mapping data of Baden-Württemberg, Matthias Albert for valuable comments, and

Robert Larkin for language revision. The constructive comments of two anonymous reviewers were greatly appreciated.

Author contributions MS and TZ conceived and designed the study. HSR and TZ developed statistical modelling approaches. TZ processed and modelled the data. CJ and DS contributed gust speed data. MJI contributed remote sensing data. TZ drafted the first manuscript. All authors participated in editing, revision, and final approval of the manuscript.

Funding Open Access funding enabled and organized by Projekt DEAL. This work was supported by the FNR (Fachagentur Nachwachsende Rohstoffe e.V.) within the framework of the Forest and Climate Fund (MiStriKli 22W-K-4-166-02).

Availability of data and materials The datasets generated during and/or analysed during the current study are available in the Zenodo Repository, <https://doi.org/10.5281/zenodo.7785331>.

Declarations

Conflict of interest The authors declare they have no conflicts of interests.

Open Access This article is licensed under a Creative Commons Attribution 4.0 International License, which permits use, sharing, adaptation, distribution and reproduction in any medium or format, as long as you give appropriate credit to the original author(s) and the source, provide a link to the Creative Commons licence, and indicate if changes were made. The images or other third party material in this article are included in the article's Creative Commons licence, unless indicated otherwise in a credit line to the material. If material is not included in the article's Creative Commons licence and your intended use is not permitted by statutory regulation or exceeds the permitted use, you will need to obtain permission directly from the copyright holder. To view a copy of this licence, visit <http://creativecommons.org/licenses/by/4.0/>.

References

- Albrecht AT, Jung C, Schindler D (2019) Improving empirical storm damage models by coupling with high-resolution gust speed data. *Agric For Meteorol* 268:23–31. <https://doi.org/10.1016/j.agrfor.2018.12.017>
- Bonnesoeur V, Constant T, Moulia B et al (2016) Forest trees filter chronic wind-signals to acclimate to high winds. *New Phytol* 210(3):850–860. <https://doi.org/10.1111/nph.13836>
- Brezger A, Lang S (2006) Generalized structured additive regression based on Bayesian P-splines. *Comput Stat Data Anal* 50(4):967–991
- Brüchert F, Gardiner B (2006) The effect of wind exposure on the tree aerial architecture and biomechanics of Sitka spruce (*Picea sitchensis*, Pinaceae). *Am J Bot* 93(10):1512–1521. <https://doi.org/10.3732/ajb.93.10.1512>
- Bürkner PC (2017) brms: an R package for Bayesian multilevel models using stan. *J Stat Sof* 80:1. <https://doi.org/10.18637/jss.v080.i01>
- Bürkner PC (2018) Advanced Bayesian multilevel modeling with the R package brms. *R J* 10(1):395. <https://doi.org/10.32614/rj-2018-017>
- Byrne KE, Mitchell SJ (2012) Testing of WindFIRM/ForestGALES_{BC}: a hybrid-mechanistic model for predicting windthrow in partially harvested stands. *Forestry* 86(2):185–199. <https://doi.org/10.1093/forestry/cps077>

- Carpenter B, Gelman A, Hoffman MD et al (2017) Stan: A probabilistic programming language. *J Stat Softw.* <https://doi.org/10.18637/jss.v076.i01>
- Clayton DG, Bernardinelli L, Montomoli C (1993) Spatial correlation in ecological analysis. *Int J Epidemiol* 22(6):1193–1202. <https://doi.org/10.1093/ije/22.6.1193>
- Copernicus (2020) Copernicus DEM - Copernicus Digital Elevation Model. https://spacedata.copernicus.eu/documents/20126/0/GEO1988-CopernicusDEM-SPE-002_ProductHandbook_I1.00.pdf, product handbook, accessed 2021/11/04
- Dupont E, Wood SN, Augustin NH (2022) Spatial+: a novel approach to spatial confounding. *Biometrics.* <https://doi.org/10.1111/biom.13656>
- Dupont S, Pivato D, Brunet Y (2015) Wind damage propagation in forests. *Agric For Meteorol* 214–215:243–251. <https://doi.org/10.1016/j.agrformet.2015.07.010>
- Gardiner B (2021) Wind damage to forests and trees: a review with an emphasis on planted and managed forests. *J For Res* 26(4):248–266. <https://doi.org/10.1080/13416979.2021.1940665>
- Gardiner B, Peltola H, Kellomäki S (2000) Comparison of two models for predicting the critical wind speeds required to damage coniferous trees. *Ecol Model* 129(1):1–23. [https://doi.org/10.1016/s0304-3800\(00\)00220-9](https://doi.org/10.1016/s0304-3800(00)00220-9)
- Gardiner B, Byrne K, Hale S et al (2008) A review of mechanistic modelling of wind damage risk to forests. *Forestry* 81(3):447–463. <https://doi.org/10.1093/forestry/cpn022>
- Gardiner B, Berry P, Moulia B (2016) Review: wind impacts on plant growth, mechanics and damage. *Plant Sci* 245:94–118. <https://doi.org/10.1016/j.plantsci.2016.01.006>
- Gelman A, Hill J (2007) *Data analysis using regression and multilevel/hierarchical models.* Cambridge University Press, Cambridge
- Gelman A, Carlin JB, Stern HS et al (2013) *Bayesian data analysis.* Chapman and Hall/CRC, Boca Raton. <https://doi.org/10.1201/b16018>
- Hale SE, Gardiner B, Peace A et al (2015) Comparison and validation of three versions of a forest wind risk model. *Environ Model Softw* 68:27–41. <https://doi.org/10.1016/j.envsoft.2015.01.016>
- Hanewinkel M, Hummel S, Albrecht A (2010) Assessing natural hazards in forestry for risk management: a review. *Eur J For Res* 130(3):329–351. <https://doi.org/10.1007/s10342-010-0392-1>
- Hart E, Sim K, Kamimura K et al (2019) Use of machine learning techniques to model wind damage to forests. *Agric For Meteorol* 265:16–29. <https://doi.org/10.1016/j.agrformet.2018.10.022>
- Jackson T, Shenkin A, Moore J et al (2019) An architectural understanding of natural sway frequencies in trees. *J R Soc Interface* 16(155):20190,116. <https://doi.org/10.1098/rsif.2019.0116>
- Jung C, Schindler D (2019) Historical winter storm atlas for Germany (GeWiSA). *Atmosphere* 10(7):387. <https://doi.org/10.3390/atmos10070387>
- Jung C, Schindler D (2021) Does the winter storm-related wind gust intensity in Germany increase under warming climate?—a high-resolution assessment. *Weather Clim Extremes* 33(100):360. <https://doi.org/10.1016/j.wace.2021.100360>
- Kamimura K, Gardiner B, Dupont S et al (2016) Mechanistic and statistical approaches to predicting wind damage to individual maritime pine (*Pinus pinaster*) trees in forests. *Can J For Res* 46(1):88–100. <https://doi.org/10.1139/cjfr-2015-0237>
- Kamimura K, Gardiner B, Dupont S et al (2019) Agent-based modelling of wind damage processes and patterns in forests. *Agric For Meteorol* 268:279–288. <https://doi.org/10.1016/j.agrformet.2019.01.020>
- Kändler G (2009) The design of the second German national forest inventory. In: McRoberts RE, Reams GA, Van Deusen PC, McWilliams WH (eds) *Proceedings of the eighth annual forest inventory and analysis symposium*; Monterey, CA. Gen. Tech. Report WO-79. Washington, DC: US Department of Agriculture, Forest Service. 19–24
- Lappi J (1997) A longitudinal analysis of height/diameter curves. *For Sci* 43(4):555–570. <https://doi.org/10.1093/forestscience/43.4.555>
- Lemoine NP (2019) Moving beyond noninformative priors: why and how to choose weakly informative priors in Bayesian analyses. *Oikos* 128(7):912–928. <https://doi.org/10.1111/oik.05985>
- Messier C, Puettmann K, Filotas E et al (2016) Dealing with non-linearity and uncertainty in forest management. *Curr For Rep* 2(2):150–161. <https://doi.org/10.1007/s40725-016-0036-x>
- de Miguel S, Mehtätalo L, Shater Z et al (2012) Evaluating marginal and conditional predictions of taper models in the absence of calibration data. *Can J For Res* 42(7):1383–1394. <https://doi.org/10.1139/x2012-090>
- Moore J, Gardiner B, Sellier D (2018) Tree mechanics and wind loading. In: Geitmann A, Gril J (eds) *Plant biomechanics.* Springer, Cham. pp. 79–106. https://doi.org/10.1007/978-3-319-79099-2_4
- Muñoz-Sabater J, Dutra E, Agustí-Panareda A et al (2021) ERA5-land: a state-of-the-art global reanalysis dataset for land applications. *Earth Syst Sci Data* 13(9):4349–4383. <https://doi.org/10.5194/essd-13-4349-2021>
- Pavlou M, Ambler G, Seaman S et al (2015) A note on obtaining correct marginal predictions from a random intercepts model for binary outcomes. *BMC Med Res Methodol.* <https://doi.org/10.1186/s12874-015-0046-6>
- Peltola H, Kellomäki S, Väisänen H et al (1999) A mechanistic model for assessing the risk of wind and snow damage to single trees and stands of Scots pine, Norway spruce, and birch. *Can J For Res* 29(6):647–661. <https://doi.org/10.1139/x99-029>
- R Core Team (2021) *R: a language and environment for statistical computing.* R Foundation for Statistical Computing, Vienna, Austria, <https://www.R-project.org/>
- Robin X, Turck N, Hainard A et al (2011) pROC: an open-source package for R and S+ to analyze and compare ROC curves. *BMC Bioinform* 12:77
- Saborowski J, Marx A, Nagel J et al (2010) Double sampling for stratification in periodic inventories—finite population approach. *For Ecol Manage* 260(10):1886–1895. <https://doi.org/10.1016/j.foreco.2010.08.035>
- Schmidt M (2009) Ein longitudinales Höhen-Durchmesser Modell für Fichte in Deutschland. In: Nagel J (ed) *Deutscher Verband Forstlicher Forschungsanstalten. Sektion Ertragskunde. Jahrestagung 25–27. Mai 2009, Ascona.* http://sektionertragskunde.fvabw.de/band2009/Tag2009_08.pdf
- Schmidt M (2020) Standortssensitive und kalibrierbare Bonitätsfächer: Wachstumspotenziale wichtiger Baumarten unter Klimawandel. *Allgemeine Forst- und Jagdzeitung* 190(5/6):136–160
- Schmidt M, Hanewinkel M, Kändler G et al (2010) An inventory-based approach for modeling single-tree storm damage—experiences with the winter storm of 1999 in southwestern Germany. *Can J For Res* 40(8):1636–1652. <https://doi.org/10.1139/X10-099>
- Scott RE, Mitchell SJ (2005) Empirical modelling of windthrow risk in partially harvested stands using tree, neighbourhood, and stand attributes. *For Ecol Manage* 218(1–3):193–209. <https://doi.org/10.1016/j.foreco.2005.07.012>
- Seidl R, Schelhaas MJ, Rammer W et al (2014) Increasing forest disturbances in Europe and their impact on carbon storage. *Nat Clim Chang* 4(9):806–810. <https://doi.org/10.1038/nclimate2318>
- Skrondal A, Rabe-Hesketh S (2009) Prediction in multilevel generalized linear models. *J R Stat Soc A Stat Soc* 172(3):659–687. <https://doi.org/10.1111/j.1467-985x.2009.00587.x>
- Suvanto S, Peltoniemi M, Tuominen S et al (2019) High-resolution mapping of forest vulnerability to wind for disturbance-aware forestry. *For Ecol Manage* 453(117):619. <https://doi.org/10.1016/j.foreco.2019.117619>

- Vehtari A, Gelman A, Gabry J (2017) Practical Bayesian model evaluation using leave-one-out cross-validation and WAIC. *Stat Comput* 27:1413–1432. <https://doi.org/10.1007/s11222-016-9696-4>
- Warrach-Sagi K, Mohr V, Wulfmeyer V (2018) High resolution WRF simulations for climate change studies in Germany. In: Nagel WE, Kröner DH, Resch MM (eds) *High performance computing in science and engineering '17*. Springer International Publishing, Cham, pp 431–440
- Wernli H, Dirren S, Liniger MA et al (2002) Dynamical aspects of the life cycle of the winter storm ‘Lothar’ (24–26 December 1999). *Q J R Meteorol S J Atmos Sci Applied Meteorol Phys Oceanogr* 128(580):405–429
- Wood S (2017) *Generalized additive models: an introduction with R*, 2nd edn. Chapman and Hall/CRC, Boca Raton

Publisher's Note Springer Nature remains neutral with regard to jurisdictional claims in published maps and institutional affiliations.